Modeling Earth Systems and Environment (2021) 7:1693–1701
https://doi.org/10.1007/s40808-020-00904-9

ORIGINAL ARTICLE

Seismic modelling study of CO_2 effects on P-wave amplitude

Aniekan M. Ekanem[1] · Nyakno J. George[1] · Jewel E. Thomas[1] · Nsikak E. Ekpenyong[2]

Received: 25 April 2020 / Accepted: 18 July 2020 / Published online: 25 July 2020
© Springer Nature Switzerland AG 2020

Abstract

The presence of carbon dioxide (CO_2) in the pores of rocks can cause changes in the amplitude of a propagating seismic wave. These changes in turn can be used to estimate the degree of saturation of this greenhouse gas in the rocks. In this paper, we examine the effects of CO_2 on P-wave amplitude in a layered medium through seismic modelling. Our hypothetical model consists of four isotropic layers. The third layer, which is our target layer, is modelled as a fully poro-elastic medium saturated with brine and CO_2 with varying crack densities. The CO_2 and brine saturations in the third layer range from 0 to 100% with crack densities of 0.01, 0.02 and 0.03, respectively. We analysed the reflection amplitudes from the top and bottom of the target layer for the case of no fluid saturation and varying degrees of saturation, respectively, in the layer. The P-wave amplitude is shown to be sensitive to the degree of CO_2 saturation and crack density. At a given crack density, the amplitude change increases with decreasing percentage of CO_2 saturation and reaches a maximum value at 5% saturation with sharp variations between 5 and 30%. The amplitude change also increases with crack density. These findings provide more valuable insights into the use of P-wave amplitude as a potential tool to obtain valuable information on reservoir fluid properties.

Keywords Amplitude · Brine · CO_2 · Bulk modulus · Fluid saturation

Introduction

In recent times, underground storage of CO_2 is considered a possible technique of reducing and stabilizing the discharge of this greenhouse gas into the atmosphere (Ravazzoli and Gomez 2014; Dupuy et al. 2017; Maurya and Singh 2019). Sometimes, CO_2 is purposely injected into hydrocarbon reservoirs to improve the rates of production and sweep efficiencies (Hendriks and Blok 1993; Bachu 2003; Ekanem et al. 2016; Shelton et al. 2016) and later stored in the reservoirs and deep saline aquifers as a way of extenuating climate change (Picotti et al. 2012; Ravazzoli and Gomez 2014; Raza et al. 2018). In the reservoir, the density of the stored CO_2 is dependent on the reservoir depth, effective porosity, pressure and local geothermal gradient (Hendriks and Blok 1993). CO_2 is equally a natural component of the hydrocarbon reservoirs with saturations ranging from 2 to 80% (van der Meer 2005; Roberts 2009; Huang et al. 2015). It exists in the gaseous state at surface pressures and temperatures but shows evidence of supercritical behaviour at a pressure of 7.38 MPa and temperature of 31.1 °C, otherwise referred to as the critical point (van der Meer 2005; David et al. 2008; Ravazzoli and Gomez 2014; Nikolai et al. 2019). Above this point, CO_2 is compressible like a gas but has the density of a liquid (van der Meer 2005; Ravazzoli and Gomez 2014).

A seismic wave propagating in the Earth gradually loses energy due to a number of factors. This loss in energy results in changes noticed in the wave amplitude, which may be related with changes in subsurface geology especially when all the other factors affecting seismic wave amplitude have been taken into account. The key factors affecting the amplitude of seismic waves propagating in a given medium are geometrical spreading, energy partitioning at interfaces, absorption and attenuation, topography of the interfaces and curvature and dipping of reflectors, source and receiver array response, scattering in the near surface and interference due to fine layering (Sheriff 1975). Another common cause of loss in seismic wave amplitude in fluid saturated rocks is the 'squirt flow' mechanism caused by wave propagation in the rocks (O'Connell and Budiansky 1977; Mavko and Nur 1979; Chapman 2003). When a seismic wave travels through

✉ Aniekan M. Ekanem
anny4mart@yahoo.com; aniekanekanem@aksu.edu.ng

[1] Department of Physics, Geophysics Research Group (GRG), Akwa Ibom State University, Mkpat Enin, Nigeria

[2] Department of Physics, Akwa Ibom State University, Mkpat Enin, Nigeria

rocks, pressure gradients are produced, which could be away from the direction of travel of the wave. Fluid then flows from the more compliant parts of the pore space into the stiffer parts along the pressure gradient during compression and back again during dilatation, a phenomenon known as 'squirt flow'. The loss in seismic wave amplitude is often quantified through the attenuation factor. Chapman (2003) developed a poro-elastic model which predicts that the attenuation factor depends on the incidence angle or offset as well as the source–receiver azimuth. The presence of a gas in the pores of the rocks can have great effects on the velocity and amplitude of the seismic wave propagating in the rocks depending on the level of saturation, porosity, permeability and frequency (White 1975; Rubino et al. 2012). Significant changes can occur in the seismic wave properties such as velocity, travel time, amplitude and attenuation when CO_2 is present in the reservoir either in the gaseous or supercritical state at various levels of saturation. Consequently, a fuller understanding of the effects of CO_2 on seismic response could be of great significance in the study of reservoir fluid properties. For example, studies by Davis et al. (2003) revealed that CO_2 can cause a percentage change of between 4 and 6% in P-wave velocity and 5 and 10% in S-wave velocity. Many studies including time-lapse studies for monitoring CO_2 sequestration in the subsurface have all revealed the sensitivity of the P- and S-wave velocities to the presence of CO_2 (e.g., Arts et al. 2004; Chadwick et al. 2005; David et al. 2008; Amir and Landro 2009; Raza et al. 2018; Agofack et al. 2018). Studies by David et al. (2008) revealed a non-linear relationship between P-wave velocity and CO_2 saturation. Their results show that P-wave velocity exhibits a remarkable decrease between 0 and 30% CO_2 saturation for the supercritical fluid case. Beyond this percentage of saturation, they observed no significant changes in the velocity. However, for the supercritical gas case, a very strong decrease occurs in the P-wave velocity at small CO_2 saturations of $< 5–10\%$ with sparse or no variation at higher levels of saturation. Becquey et al. (2010) reported from their modelling studies to evaluate the seismic effects of CO_2 injected into a partially depleted oil field, the observation of small time lapse effects, including 0.4 ms time shifts and 4–6% amplitude change. Ravazzoli and Gomez (2014) in their study to analyse the seismic amplitude variation with azimuth (AVA) and model the behaviour of intercept, gradient and curvature attributes at varying levels of CO_2 saturation, reported a monotonic increase in magnitude of the intercept which obviously shows a decrease in the acoustic impedance for increasing CO_2 saturation. Dupuy et al. (2017) in their study to obtain CO_2 elastic properties using a model based amplitude variation with offset (AVO) inversion reported that it is difficult to discriminate between high CO_2 saturations. Despite the intensive effort in research and development, there is still a lack of fuller understanding of the effects that CO_2 might have on seismic wave amplitude especially at varying percentages of saturation. A synthetic modelling study approach could add more helpful insights into the effects of CO_2 on seismic response particularly on seismic amplitude and thus, afford a physical basis of using this seismic attribute for getting valuable information on the reservoir fluid characteristics. Thus, in this paper, the effects of CO_2 held in the pore space of the rock on seismic wave amplitude are examined through synthetic modelling. Our main aim is to study the changes that the presence of CO_2 at varying level of saturation might cause on P-wave amplitude in a layered medium with randomly aligned micro-cracks.

Materials and methods

Hypothetical model

The hypothetical model consists of four isotropic and horizontal layers as shown in Fig. 1. The third layer contains a porous fluid-saturated material and squirt flow in the matrix is taken into account. The porous material is saturated with CO_2 in the supercritical state and brine at varying amount of concentrations to study the effects that CO_2 might have on seismic wave amplitude propagating in the model. The Chapman's poro-elastic model (2003) was used to compute the elastic properties of the porous material in the target layer. According to Chapman's model (2003), the pore space of the rock consists of a lattice arrangement of spherical pores, aligned ellipsoidal fractures and randomly oriented ellipsoidal micro-cracks. Detailed description of this model is well documented in Chapman (2003). We set the fracture density in the model to zero to study the effect of fluid

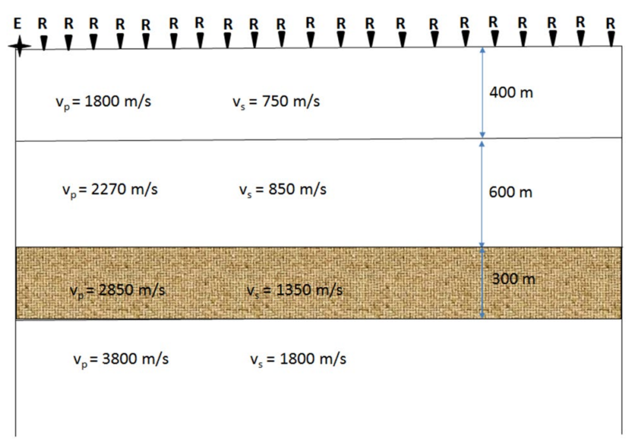

Fig. 1 Hypothetical model and experimental set-up. The model consists of four horizontal layers. The third layer is saturated with brine and CO_2 at varying percentages and contains micro-cracks. *E* is the explosive source placed on the surface of the model, while *R* is the receiver. The receiver spacing is 100 m

saturation in a porous medium with no fractures. The average bulk modulus of brine was taken as 2.305 GPa while that of CO_2 was taken as 0.008 Gpa. Porosity was taken as 37%. The values of these parameters were based on the data obtained from the Sleipner field in the North Sea (Chadwick et al. 2005) to provide a more practical situation for the seismic modelling study. The major aquifer in the field is the Utsira Sand and several millions of tonnes of CO_2 have been injected into the Sand since 1996 (Chadwick et al. 2005; Bickle et al. 2007; Arts et al. 2008) as part of the measures to lessen greenhouse gas effect. The CO_2 in the reservoir, whose thickness ranges from 200 to 300 m, exists in the supercritical state. Details of the hypothetical model parameters are given in Fig. 1.

With the homogeneous mixing of CO_2 and brine in the pores and micro-cracks of the third layer, the effective fluid bulk modulus K_{eff} is given by the Wood's formula (Mavko et al. 2009):

$$\frac{1}{K_{\mathrm{eff}}} = \frac{S_{\mathrm{b}}}{K_{\mathrm{b}}} + \frac{1 - S_{\mathrm{b}}}{K_{\mathrm{c}}}, \tag{1}$$

where S_b and K_b are the percentage of brine saturation and the bulk modulus of brine respectively, and K_c is the bulk modulus of CO_2. Wood's formula (Eq. 1) is only appropriate for the low frequency limit, in which the pressure gradients have adequate time to relax and stabilize. This stabilized state is attained because of the smaller relaxation times associated with the grain scale considered in the hypothetical model.

Experimental set-up and computation of synthetic data

Synthetic data were computed for the hypothetical model with the use of a commercial software called ANISEIS. This software makes use the reflectivity method to model seismic wave propagation in anisotropic media and is a far field approximation (Taylor 2001). First, we computed synthetic data for the case of a pure isotropic model with no fluid saturation, no micro-cracks and no porosity in the third layer to provide a reference. CO_2 in the supercritical state and brine were then introduced into the third layer at brine saturation percentages varying from 0 to 100% and crack densities of 0.01, 0.02 and 0.03, respectively, to investigate the effects of the partial saturation on P-wave amplitude. The CO_2 saturation (S) in this case is given as:

$$S = 1 - S_{\mathrm{b}}. \tag{2}$$

100% CO_2 saturation means that the material is completely saturated with CO_2, while 0% CO_2 saturation implies that the material is wholly saturated with brine. The bulk modulus of CO_2 will significantly control the effective fluid bulk moduli at low percentages of brine saturation and vice versa as evidenced from Eq. (1).

We used an explosive source placed on the surface of the hypothetical model as our seismic source. This source generates a Ricker wavelet with a centre frequency of 25 Hz as the source wavelet. The modelling software adjusts the explosive source in such a way that only the contribution of the waves directed into the model are produced while the outward components of the waves are suppressed (Taylor 2001). 21 receivers were placed on the surface of the model to record the resulting wave field with a constant spacing of 100 m. Recording was done with a time step of 1 ms and a net sampling time of 3 s. Figure 2 shows a sample synthetic data for the model with CO_2 saturation of 10% and crack density of 0.02 in the target layer. The reflections from the top and bottom of the target layer are indicated in the figure by the blue and red arrows, respectively. The event indicated by the red ellipse is the P-S converted wave, which was not analysed in this study. Only the effect of changes in fluid bulk modulus is considered in this study.

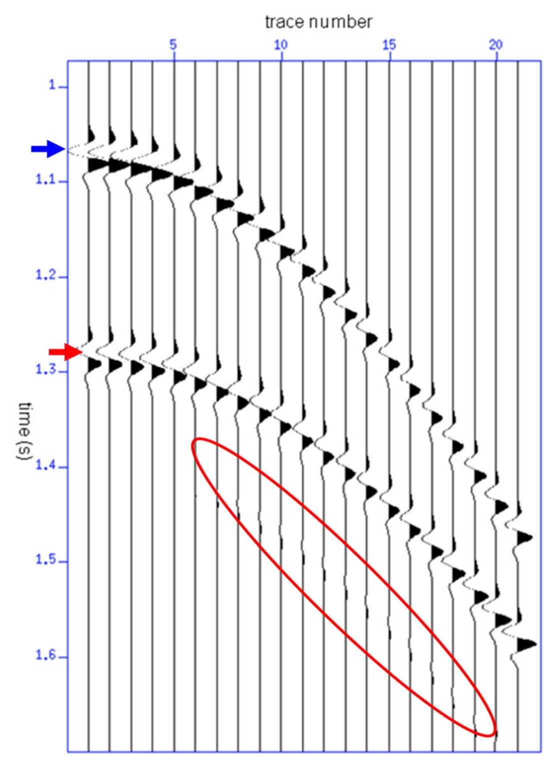

Fig. 2 Sample synthetic data for model with 10% CO_2 saturation and 0.02 crack density in the third layer. The blue and red arrows point to the top and bottom of the reflections from the third layer while the red ellipse is the P-S converted wave. The separation of the traces is 100 m

Data analysis and results

The reflections from the top and bottom of the third layer of the hypothetical model for both the isotropic and fluid saturated cases were computed using the Fast Fourier Transform (FFT) algorithm, respectively, with a constant time window of 160 ms. Figure 3 shows sample plots of the times series of the target layer's top and bottom reflections at 400 m and 1000 m offsets for the three crack densities considered. There is no significant difference in the reflection amplitudes for the top layer for the two offsets and crack densities considered (Fig. 3). This of course is as expected, since the first two layers are isotropic. Significant variations in amplitude are observed for the two offsets shown and crack densities for the bottom layer reflection. The amplitude decreases with increasing crack density and offset. These observations demonstrate the sensitivity of the seismic wave amplitude to the varying percentages of CO_2 saturation and crack densities in the model.

The amplitude spectrum at fixed offsets of 300 m and 1500 m are shown in Fig. 4 for both the pure isotropic model and model with CO_2 saturation of 10% and crack density of 0.01, respectively. There is no difference in the peak amplitudes of the top reflections for the two cases as expected. However, changes in the peak amplitudes are noticeable for the two cases for the bottom layer reflection due the combined effect of the fluid saturation and cracks in the target layer. The peak frequencies of both the top and bottom layer reflections are observed to be higher than the centre frequency of the input Ricker wavelet because the generated far field wavelet is proportional to the derivative of the source wavelet with respect to time (Taylor 2001). The peak frequency of the Ricker wavelet and that of its time derivative are related together by (Lange and Almoghrabi 1988; Chung and Lawton 1995):

$$f_D = f_R\sqrt{\frac{3}{2}}, \quad (3)$$

where f_D is the peak frequency of the time derivative of the Ricker wavelet and f_R is the peak frequency of the Ricker wavelet. Equation (3) elucidates the increase in the peak frequency of the far field wavelet relative to the input wavelet.

Figure 5 shows the amplitude-offset profile for the isotropic model (with no fluid saturation and cracks in the target layer) and model with fluid saturation and cracks, respectively. The black colour indicates the peak amplitude of the reflection from the top of the third layer, while the blue colour indicates the peak amplitude of the bottom layer reflection. The red colour indicates the difference in the peak amplitudes between

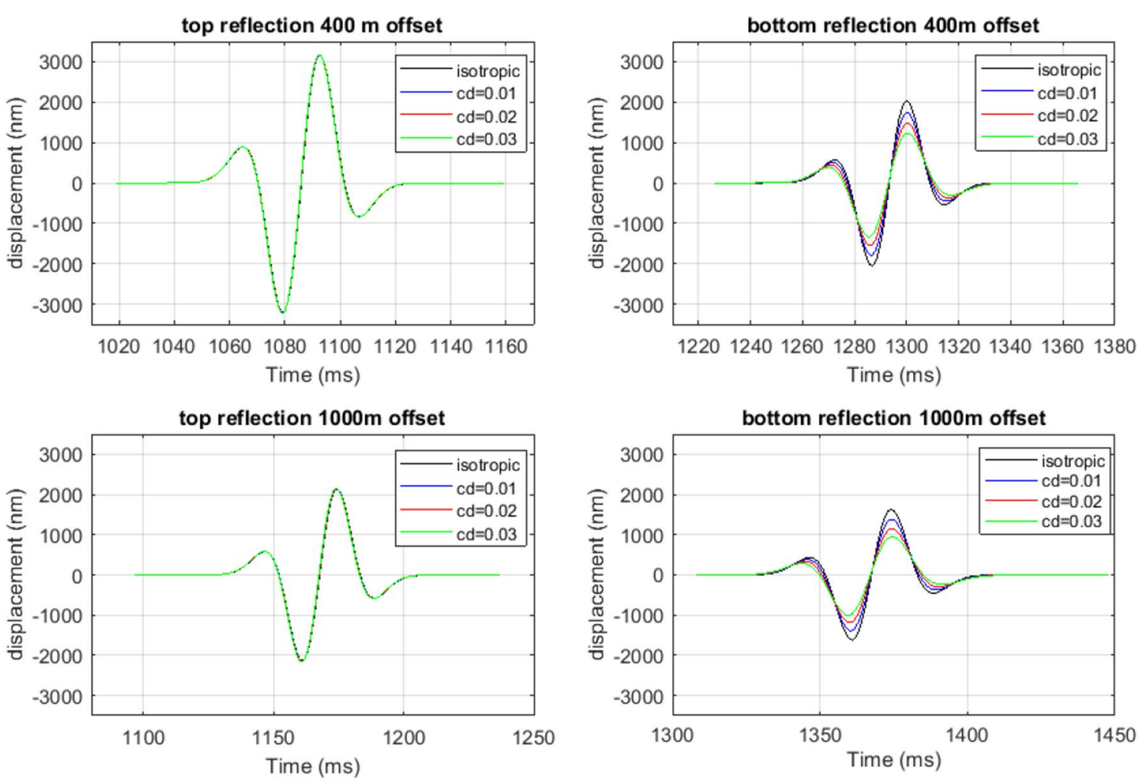

Fig. 3 Sample time series plots of the reflections from the top and bottom of the third layer reflection

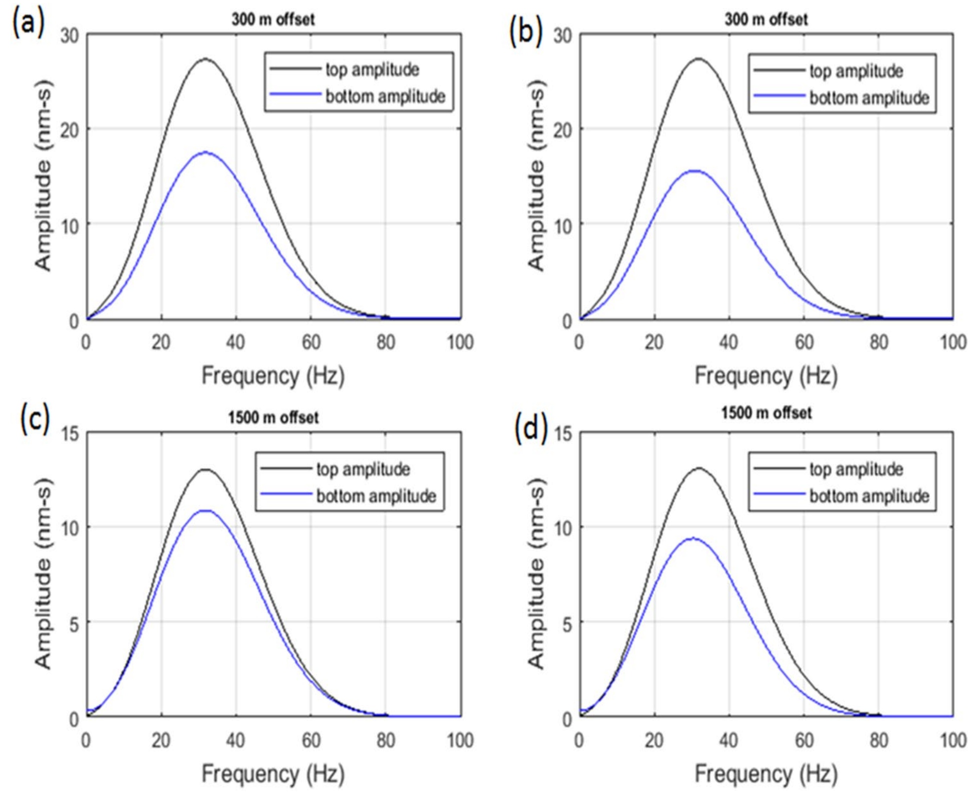

Fig. 4 Sample amplitude spectra (**a**) 300 m offset for pure isotropic model. (**b**) 300 m offset for 10% CO_2 saturation and crack density of 0.01. (**c**) 1500 m offset for pure isotropic model. (**d**) 1500 m offset for 10% CO_2 saturation and crack density of 0.01

the top and bottom layer reflections. The amplitudes vary with increasing offsets or incidence angles according to Zoeppritz equations. AVO effects as well as geometrical spreading effects are noticeable on all the profiles as amplitude decreases with offset and distance or depth of wave propagation. For the pure isotropic model, the difference in the peak amplitudes dA1 is due to the combine effects of AVO and geometrical spreading. However, for the model with fluid saturation and cracks, the difference in peak amplitudes dA2 is due to the combined effects of AVO, geometrical spreading, CO_2 saturation and the embedded cracks. This amplitude difference (dA2) increases with increasing crack density as shown in the profiles. To investigate the effects of fluid saturation and crack density on the seismic wave amplitude, the effect of the geometrical spreading factor and AVO effects were eliminated by taking the difference between dA1 and dA2, respectively. This amplitude difference is denoted as dA_S (Fig. 6). The resultant change in amplitude profiles are shown in Fig. 6 for the three crack densities considered in this study. The plots show a direct relationship between the change in amplitude and crack density for the given percentage of CO_2 saturation (10%). The amplitude difference or amplitude change at 10% percentage of CO_2 saturation is approximately constant for the various offsets from 0 to 1500 m. Figure 7 illustrates the combined effects of CO_2 saturation and crack density on the P-wave amplitude. The amplitude change dA_S increases with crack density as shown in the 3D plot of Fig. 7. At a given percentage of CO_2 saturation, the amplitude difference remains constant, which is indicative of the fact that both AVO and geometrical spreading effects are absent. The magnitude of the amplitude difference is dependent on the degree of CO_2 saturation as seen in Figs. 7 and 8. Higher magnitudes of amplitude difference are obtained in the fluid-saturated layer at 0% CO_2 saturation or 100% brine saturation and lower values of amplitude difference at 100% CO_2 or 0% brine saturation for the three crack densities considered (Figs. 7, 8). The magnitudes of the amplitude difference are observed to increase steadily with decreasing percentages of CO_2 saturation from 100 to 5% for a given crack density where there is a peak in the values of the amplitude difference or amplitude change. This implies that the P-wave loses more energy as the percentage of CO_2 saturation decreases. A remarkable change in the amplitude difference is observed for CO_2 saturations of between 5 and 30%. Beyond this limit of saturation, there is a subtle and gradual decrease in the magnitude of the amplitude change with increasing percentage of CO_2 saturation.

Discussion and concluding remarks

Seismic wave amplitude depends among other factors on the nature and degree of the fluid saturation in the pores of the rock. The poro-elastic model of Chapman (2003) has been used in this study to examine the effects of CO_2 saturation

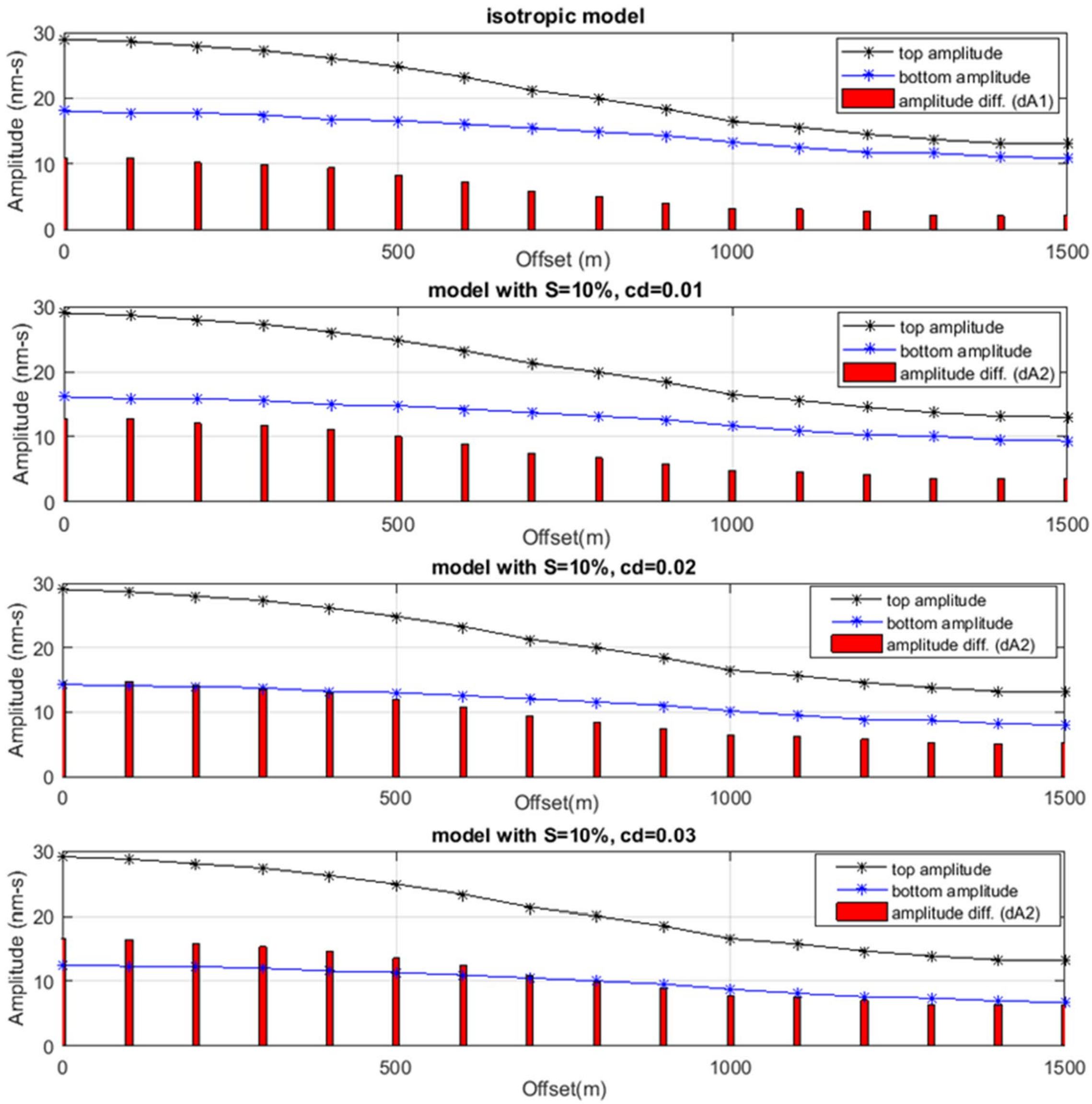

Fig. 5 Amplitude-offset profile. The black colour indicates third layer top reflection while the blue colour indicates the bottom layer reflection. The red colour indicates the difference in the peak amplitude between the top and bottom layer reflections. dA1 is the difference in the peak amplitudes of the top and bottom reflections for the pure isotropic model, while dA2 is the difference in the peak amplitudes of the top and bottom reflections for the model with fluid saturation and cracks

at varying percentages on P-wave amplitude. The CO_2 is assumed to be in the supercritical state and the CO_2 properties at the Sleipner gas field in the North Sea are used in the modelling for simplicity and to provide a more realistic reservoir model. The results of this study demonstrate that P-wave amplitude is sensitive to the uniform saturation of the pores and cracks in the target layer of the hypothetical model. Uniform saturation of CO_2 and brine in this case causes changes in the density, viscosity and the effective bulk modulus (Chapman and Liu 2006; Maultzsch et al. 2003; David et al. 2008). Consequently, the amplitude of the seismic wave propagating through the fluid-saturated layer is affected by these changes, which are dependent on the degree of saturation of the fluids. The P-wave amplitude has been proved to be very sensitive to the degree of CO_2 saturation. More amplitude changes occur when the target layer is completely saturated with CO_2 (i.e., 100% CO_2 saturation) than when the layer is completely saturated with brine (i.e., 0% CO_2 saturation). The implication of this is that the presence of CO_2 in the saturated layer causes more loss in seismic wave energy than brine. A possible explanation for this is that CO_2 behaves as a liquid at the supercritical phase which is assumed in the hypothetical model. Crack density is also seen to affect the amplitude of

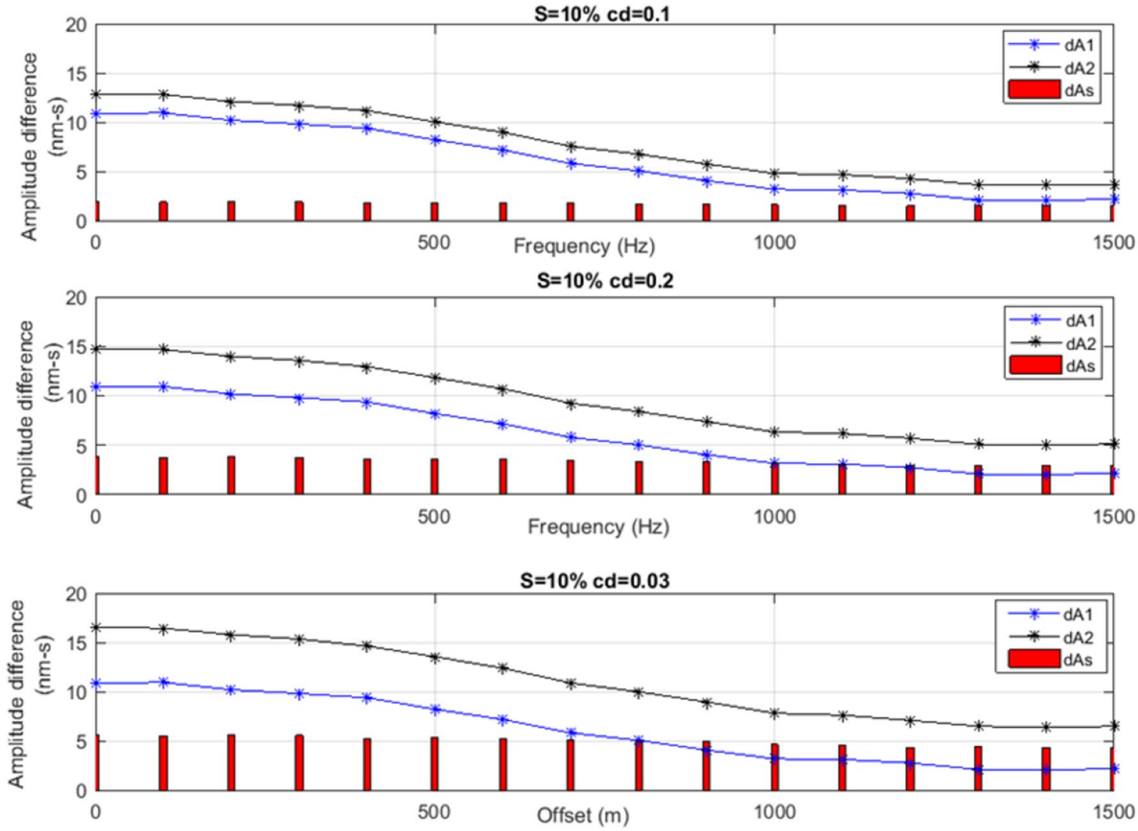

Fig. 6 Effect of crack density on P-wave amplitude. Increasing crack density leads to increase in the amplitude difference. dA1 is the difference in the peak amplitudes of the top and bottom reflections for the pure isotropic model, while dA2 is the difference in the peak amplitudes of the top and bottom reflections for the model with fluid saturation and cracks. dAs is the amplitude change caused by fluid saturation and cracks and is the difference between dA1 and dA2

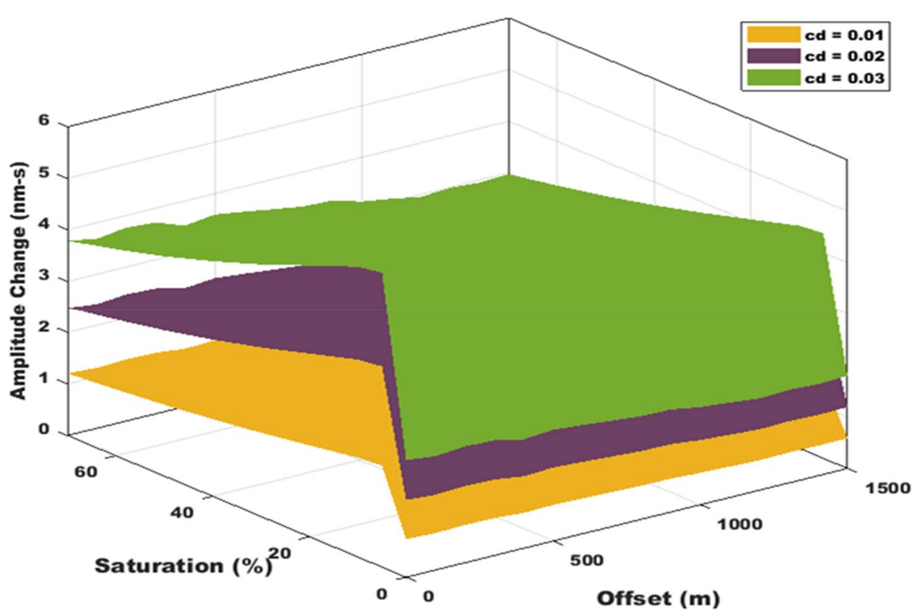

Fig. 7 3D plot of amplitude change against CO_2 saturation for different degrees of saturations and offsets. The magnitude of the amplitude change increases steadily with decreasing degree of CO_2 saturation and increasing crack density and reaches a maximum around 5% of CO_2 saturation

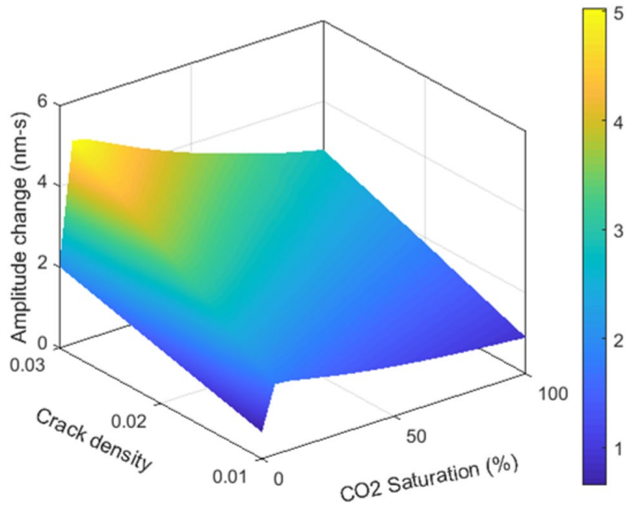

Fig. 8 3D plot of amplitude change against CO_2 saturation for different degrees of saturations and crack densities. There is a systematic increase in the magnitude of the amplitude change with decreasing percentage of CO_2 saturation with a maximum value around CO_2 saturation of 5% for the three crack densities considered

the propagating seismic wave in the fluid saturated layer. The amplitude change increases with increasing crack density which is also indicative of more loss in seismic wave energy with increasing crack density. Significant variations occur in the amplitude change between 5 and 30% of CO_2 saturation and subsequently, only very small and steady variations occur. Comparing the results of this study to that of David et al. (2008); it can be concluded that the P-wave amplitude is more sensitive to the degree of CO_2 saturation than velocity, particularly at higher percentages of saturations. These findings are also consistent with the results of the study conducted by Ekanem et al. (2016) which demonstrated the sensitivity of seismic wave attenuation to CO_2 saturation. A common measure of the amplitude changes during seismic wave propagation in a given porous saturated medium is the attenuation factor which occurs due to the relaxation of the fluid-pressure gradients created by the propagation of seismic waves in the cracked and porous medium. Greater amplitude changes imply more attenuation and vice versa. Although this study is not entirely new per se, it is useful to show that the presence of CO_2 at varying degrees of saturation could cause measurable effects on the propagating seismic wave amplitude, at least for the relatively simplified hydrocarbon reservoir modelled in this study. Thus, our findings further demonstrate the sensitivity of P-wave amplitude to CO_2 saturation and provide deeper insights into the use of P-wave amplitude as a supplementary tool to obtain important information on reservoir fluid properties from seismic data. The results in particular, tender the prospect of utilizing the P-wave amplitude attribute to characterize rock formations for a series of applications which include subsurface depository of CO_2 as well as oil and gas exploration and production.

Acknowledgements The authors are grateful to Akwa Ibom State University (AKSU), Mkpat Enin, Nigeria for providing the necessary facilities to carry out this work and the Edinburgh Anisotropy Project (EAP) for also supporting the project and the permission to publish the results.

References

Agofack N, Losovyi S, Bauer A (2018) Effect of CO_2 on P-and S-wave velocities at seismic and ultrasonic frequencies. Int J Greenhouse Gas Control 78:388–399

Amir G, Landro M (2009) Estimation of thickness and velocity changes of injected carbon dioxide layers from pre-stack time-lapse seismic data. Geophysics 74(2):017–028

Arts R, Eiken O, Chadwick A, Zweigel P, van der Meer L, Zinszner B (2004) Monitoring of CO_2 injected at Sleipner using time-lapse seismic data. Energy 29:1383–1392

Arts R, Chadwick A, Eiken O, Thibeau S, Nooner S (2008) Ten years' experience of monitoring CO2 injection in the Utsira Sand at Sleipner, offshore Norway. First Break 26:65–72

Bachu S (2003) Screening and ranking of sedimentary basins for sequestration of CO_2 in geological media in response to climate changes. Environ Geol 44:277–289

Becquey M, Lucet N, Huguet F (2010) Feasibility of seismic monitoring at a potential CO_2 injection test site in the Paris Basin. Oil Gas Sci Technol 65(4):589–595

Bickle M, Chadwick A, Huppert HE, Hallworth M, Lyle S (2007) Modelling carbon dioxide accumulation at Sleipner: implications for underground carbon storage. Earth Planet Sci Lett 255:164–176

Chadwick RA, Arts S, Eiken O (2005) 4D seismic quantification of a growing CO_2 plume at Sleipner, North Sea. Petroleum Geology: North-West Europe and Global Perspectives. In: Proceedings of the 6th Petroleum Geology Conference. p 1385–1399

Chapman M (2003) Frequency-dependent anisotropy due to meso-scale fractures in the presence of equant porosity. Geophys Prospect 51:369–379

Chapman M, Liu E (2006) Seismic attenuation in rocks saturated with multi-phase fluids. In: 76th Annual International Meeting SEG Extracted Abstracts. p 1988–1992

Chung H, Lawton DC (1995) Frequency characteristics of seismic reflections from thin beds. Can J Exp Geophys 31:32–37

David L, Don A, Wright R, Dave M, Cole S (2008) Seismic monitoring of CO_2 geo-sequestration: realistic capabilities and limitations. In: 78th Annual International Meeting Extracted Abstracts SEG. p 2841–2845

Davis TL, Terrell MJ, Benson RD, Cardona R, Kendall R, Winarsky R (2003) Multicomponent seismic characterization and monitoring of CO_2 flood at Weyburn Field, Saskatchewan. Lead Edge 22:696–697

Dupuy B, Torres CVA, Ghaderia A, Querendeza E, Mezyka M (2017) Constrained AVO for CO_2 storage monitoring at Sleipner. Energy Procedia 114:3927–3936

Ekanem AM, Li XY, Chapman M, Main IG (2016) Effects of CO_2 on P-wave attenuation in porous media with micro-cracks: a synthetic modelling study. J Appl Geophys 135:309–316

Hendriks CA, Blok K (1993) Underground storage of carbon dioxide. Energy Convers Manage 34:949–957

Huang B, Tian H, Huang H, Yang J, Xiao X, Li L (2015) Origin and accumulation of CO_2 and its natural displacement of oils in the continental margin basins, northern South China Sea. AAPG Bull 99(7):1349–1369. https://doi.org/10.1306/02091514125

Lange JN, Almoghrabi HA (1988) Lithology discrimination for thin layers using wavelet signal parameters. Geophysics 53(12):1512–1519

Maultzsch S, Chapman M, Liu E, Li XY (2003) Modelling frequency-dependent seismic anisotropy in fluid-saturated rock with aligned fractures: implication of fracture size estimation from anisotropic measurements. Geophys Prospect 51:381–392

Maurya SP, Singh NP (2019) Seismic modelling of CO_2 fluid substitution in a sandstone reservoir: a case study from Alberta. Can J Earth Syst Sci 128:1–18

Mavko GM, Nur A (1979) Wave attenuation in partially saturated rocks. Geophysics 44:61–178

Mavko G, Mukerji T, Dvorkin J (2009) The rock physics handbook, 2nd edn. Cambridge University Press, Cambridge

Nikolai P, Rabiyat B, Aslan A, Ilmutdin A (2019) Supercritical CO_2: properties and technological applications—a review. J Therm Sci 28:394–430. https://doi.org/10.1007/s11630-019-1118-4

O'Connell RJ, Budiansky B (1977) Viscoelastic properties of fluid saturated cracked solids. J Geophys Res 82:5719–5735

Picotti S, Carcione JM, Gei D, Rossi G, Santos JE (2012) Seismic modelling to monitor CO_2 geological storage: the Atzbach-Schwanenstadt gas field. J Geophys Res 117:B06103. https://doi.org/10.1029/2011JB008540

Ravazzoli CL, Gomez JL (2014) Seismic reflectivity in carbon dioxide accumulations: a review: In: Carbon sequestration. chapter: Seismic reflectivity in carbon dioxide accumulations: a review. p 343–363

Raza A, Gholami R, Rezaee R, Bing CH, Nagaragan R, Hamid MA (2018) CO_2 storage in depleted gas reservoirs: a study on the effect of residual gas saturation. Petroleum 4:95–107

Roberts J (2009) Developing the rock physics model - improved carbon dioxide mixing rules for carbon capture and storage. In: 71st Conference and Technical Exhibition, EAGE, Expanded Abstract

Rubino JM, Velis DR, Hollige K (2012) Permeability effects on the seismic response of gas reservoirs. Geophys J Int 189(1):448–468. https://doi.org/10.1111/j.1365-246X.2011.05322.x

Shelton JL, McIntosh JC, Hunt AG, Beebe TL, Parker AD, Warwick PD, Drake RM, McCray JE (2016) Determining CO_2 storage potential during miscible CO_2 enhanced oil recovery: noble gas and stable isotope tracers. Int J Greenhouse Gas Contrs 51:239–253

Sheriff R (1975) Factors affecting seismic amplitudes. Geophys Prospect 23:125–138

Taylor D (2001) ANISEIS v5.2 Manual. Applied Geophysical Software Inc. Houston

van der Meer B (2005) Carbon dioxide storage in natural gas reservoirs. Oil Gas Sci Technol 60(3):527–536

White JE (1975) Computed seismic speeds and attenuation in rocks with partial gas saturation. Geophysics 40(2):224–232

Publisher's Note Springer Nature remains neutral with regard to jurisdictional claims in published maps and institutional affiliations.